

Measurement of the cosmic-ray energy spectrum with the TALE detector in hybrid mode

H. Oshima,^{a,*} K. Fujita,^a S. Ogio^a and T. Sako^a

^a*Institute for Cosmic Ray Research, the University of Tokyo,
5-1-5 Kashiwa-no-ha, Kashiwa, Chiba, Japan*

E-mail: oshima@icrr.u-tokyo.ac.jp

The TA Low-energy Extension (TALE) experiment extends the reach of the TA experiment on the low-energy side to below 10^{16} eV. A primary objective of TALE is to study the transition from galactic to extragalactic cosmic rays. The TALE detector is a hybrid observatory composed of fluorescence telescopes and a surface detector array of scintillation counters. The surface detectors are arranged with inter-counter spacing optimized for hybrid energy spectrum measurements in the low-energy region. We analyzed data collected between November 2018 and May 2023, corresponding to 1,247 hours of operation, and in this presentation, we will show the results of the cosmic ray energy spectrum measurement using the TALE hybrid detector. This measurement will play an important role in understanding the transition from cosmic rays of galactic origin to those of extragalactic origin.

39th International Cosmic Ray Conference (ICRC2025)
15–24 July 2025
Geneva, Switzerland



*Speaker

1. Introduction

More than 100 years have passed since the discovery of cosmic rays, but the origin of ultra-high energy cosmic rays (UHECRs) has not been revealed yet. Revealing the UHECR origins is one of the most important topics of cosmic-ray physics. Galactic cosmic rays originate within the Milky Way Galaxy, while extragalactic cosmic rays originate outside the galaxy. In the energy region below 10^{18} eV, galactic and extragalactic cosmic rays are in competition with each other. The shape of the energy spectrum reflects various physical phenomena such as the transition from galactic to extragalactic cosmic rays, the characteristics and acceleration limits of galactic cosmic rays, and confinement by the galactic magnetic field. To unravel the intricately intertwined information, it is essential to measure the cosmic-ray energy spectrum and the composition over a wide energy range. We cover the wide energy range of five orders of magnitude from 10^{15} eV to 10^{20} eV by both the Telescope Array (TA) [1, 2] and the TA Low-energy Extension (TALE) [3, 4] experiments. We aim to measure the acceleration limit of galactic cosmic rays through the measurements of composition and energy spectrum, and the transition from galactic to extragalactic cosmic rays using the TALE detector.

2. TALE detector and data samples

TA is the largest cosmic-ray detector in the Northern Hemisphere, located in Millard County, Utah, USA. The TALE experiment extends the energy range observed by the TA experiment to lower energies. The TALE detector is suitable for studying the energy spectrum structure and the associated change in the composition of cosmic rays below 10^{18} eV. The TALE detector is a hybrid apparatus composed of scintillation surface detectors (SDs) covering an area of approximately 20 km^2 and fluorescence telescopes (FDs) overlooking the SDs, as shown in Fig. 1. The TALE SDs are placed at 400 m and 600 m spacing for low-energy thresholds. In this study, we analyzed data samples between November 2018 and May 2023 corresponding to 1,247 hours of operation. These data are collected using both the FDs and the SDs.

3. Monte Carlo simulation

Detector aperture is evaluated using a Monte Carlo (MC) simulation. The MC simulations used in this work include the generation of extensive air showers by cosmic ray primaries and the detector response to these showers. Air-shower simulations are generated with the CORSIKA program [5] using QGSJet II-04 [6] hadronic interaction model at high energies. Air showers are generated with primary energies ranging from $10^{16.3}$ eV to $10^{18.5}$ eV. Five primaries, H, He, N, Si, and Fe, are included in the air-shower generations weighted with a relative abundance based on the H4a composition model [7]. In addition to the H4a model, we fit the distributions of the depth of shower maximum, X_{max} , measured by the TALE hybrid observation to a mixture of three primaries (H, N, and Fe) as a function of energy, and used the resulting abundances in our simulation. The primary mixture by the TALE hybrid observation is referred to as THXF [8], which is short for the TALE hybrid X_{max} distribution fit. These showers are thrown with an isotropic zenith angle distribution between 0° and 70° and a uniform azimuthal distribution between 0° and 360° . Particle

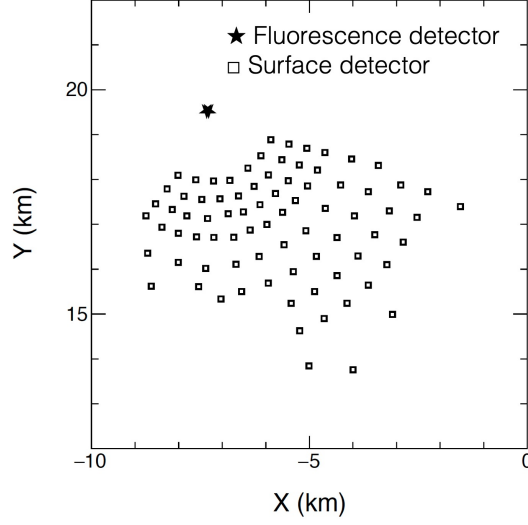


Figure 1: Physical location of the TALE detector. The TALE detector is a hybrid apparatus composed of surface detectors and fluorescence detectors.

information such as position and momentum at the detector level is used to obtain the energy deposit in each SD with the GEANT code [9–11]. The response of the SD electronics is also taken into account [12]. The FD simulation includes fluorescence and Cherenkov photon generations, telescope optics, detector calibration, and the response of the electronics.

4. Data analysis

The analysis is based on hybrid data collected by the TALE FDs and SDs. One of the advantages of hybrid observation is that the X_{\max} which is a sensitive quantity for composition analysis is measured by FDs. In addition, the SD array is used to determine the shower axis and it improves the energy resolution compared to the FD mono observation. We used events that are triggered by the FDs and have at least one SD with a signal above one minimum ionizing particle energy loss. In this analysis, we used only the upper 10 telescopes that observe fields of view at high elevation angles.

The image of the air shower observed by FDs is referred to as the event track. The following conditions are required to select event tracks that have high-quality reconstruction: 1) X_{\max} of the air shower is within the field of view of the FDs; and 2) the reduced χ^2 in the fitting of longitudinal development of the air shower is less than 3.

As the air shower develops, both the atmospheric fluorescence and the Cherenkov light are emitted. Cherenkov light is the dominant component below $10^{17.0}$ eV, while the fluorescence component increases with increasing energy, becoming the main component above $10^{17.5}$ eV. Events with a fraction of fluorescence light above 75% are defined as fluorescence events, while the others are defined as Cherenkov events. Several filtering criteria are then applied to select shower-induced track-like events. Regarding the Cherenkov events, the following conditions are required: 1) event duration is above $0.1 \mu\text{s}$; 2) the number of PMTs constituting the track is at least 10; 3) the average number of photo-electrons/PMT is greater than 50; and 4) the track length is greater than 6.5° .

Concerning the fluorescence events, the sum of the number of photo-electrons in all PMT's is required to be at least 2000 per event. In addition to these filtering conditions, the zenith angle acceptance was set to $\theta < 60^\circ$, while the energy range was set between $10^{16.9}$ eV and $10^{18.3}$ eV.

The measured energy spectrum is not an exact representation of the true energy spectrum due to the efficiency and resolution of detectors. Therefore, an unfolding is performed to correct the smearing between the true spectrum and the measured spectrum. In this analysis, we used the Iterative unfolding method proposed by D'Agostini [13, 14]. This unfolding method is based on Bayes' theorem and the unsmeared can be written as

$$C'_i = \sum_{j=1}^{N_m} U_{ij} E_j^{data}, \quad (1)$$

where C'_i is the number of true events in the i -th true energy bin, N_m is the number of bins of the measured spectrum, U_{ij} is an unsmeared matrix, and E_j^{data} is the number of events in the j -th measured energy bin. Figure 2 shows a resolution map between true and measured energies. The resolution map is evaluated by the MC simulation. Unsmeared matrix can be calculated by the resolution map. The unfolded spectrum is obtained through the unsmeared process of the measured spectrum based on the unsmeared matrix. The binning was chosen so that each bin contains a comparable number of events.

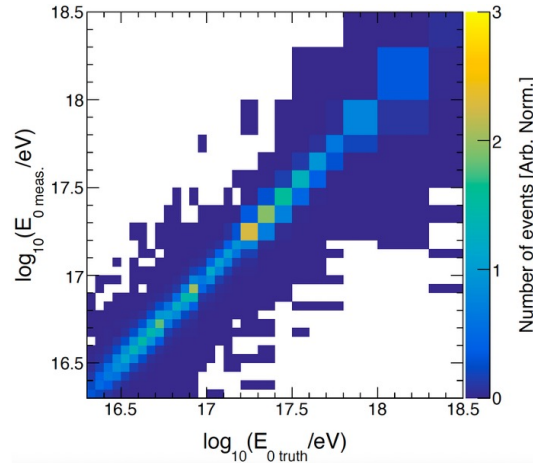


Figure 2: Resolution map between true and measured energies. The resolution map is evaluated by the MC simulation.

The product of the effective aperture and the observation time is called the effective exposure. Figure 3 shows the effective exposure used in this analysis. The effective exposure is evaluated by the MC simulation. The exposure in the high-energy region above 10^{18} eV becomes flat because the size of the ground array is fixed. The energy spectrum is expressed as

$$J(E_i) = \frac{\sum_{j=1}^{N_m} U_{ij} N_j^{sel}}{A\Omega(E_i) \cdot T \cdot \Delta E_i}, \quad (2)$$

where $J(E_i)$ is the flux in the i -th energy bin, U_{ij} is the unsmeared matrix, N_j^{sel} is the number

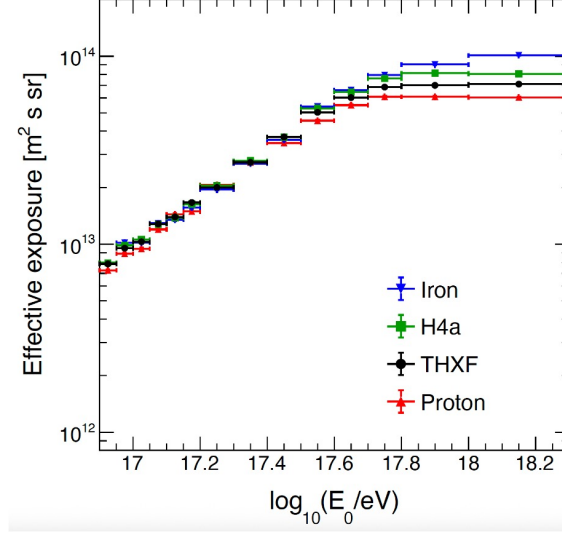


Figure 3: Effective exposure in this analysis. The effective exposure is expressed as a function of the true energy. This exposure is evaluated by the MC simulation.

of selected events in the j -th measured energy bin, $A\Omega(E_i)$ is the effective aperture, T is the observation time, and ΔE_i is the width of the i -th bin.

5. Results

Figure 4 shows the distributions of the parameters related to reconstructed shower geometrical parameters which are core positions X and Y , zenith angle, azimuth angle, Ψ angle, and R_p . The Ψ angle is the angle of the shower axis with respect to the direction of the center of the shower track and R_p is the shower impact parameter to the detector.

Figure 5 shows the energy distribution of the events. The energy resolution in the range of $10^{17.4}$ eV to $10^{17.5}$ eV is $+7.2\%/ -8.8\%$ for protons and $+6.6\%/ -6.4\%$ for iron nuclei.

Figure 6 shows the result of the energy spectrum obtained in this study, as well as that reported by the TALE FD mono observation [3]. In this analysis, the TALE hybrid observation data with the THXF composition model was used. The results of a single and a broken power-law fittings are shown in Fig. 7. The χ^2/ndf of a single power-law fitting is 21.6/12, while that of a broken power-law fitting is 21.0/10. The break point is estimated as $\log_{10}(E_{\text{break}}/\text{eV}) = 17.11 \pm 0.09$, while the spectral indices are -2.91 ± 0.10 and -3.14 ± 0.04 .

6. Summary

It is important to measure the acceleration limit of galactic cosmic rays through the measurements of composition and energy spectrum and to understand the transition from galactic to extragalactic cosmic rays. To study those physical topics, it is essential to measure the cosmic-ray energy spectrum and the composition over a wide energy range. In this work, we observed and analyzed the cosmic-ray events in the energy range of 10^{16} eV to 10^{18} eV using hybrid observations with the TALE FD and the TALE SD array with 400 m–600 m spacing. In this talk, we presented

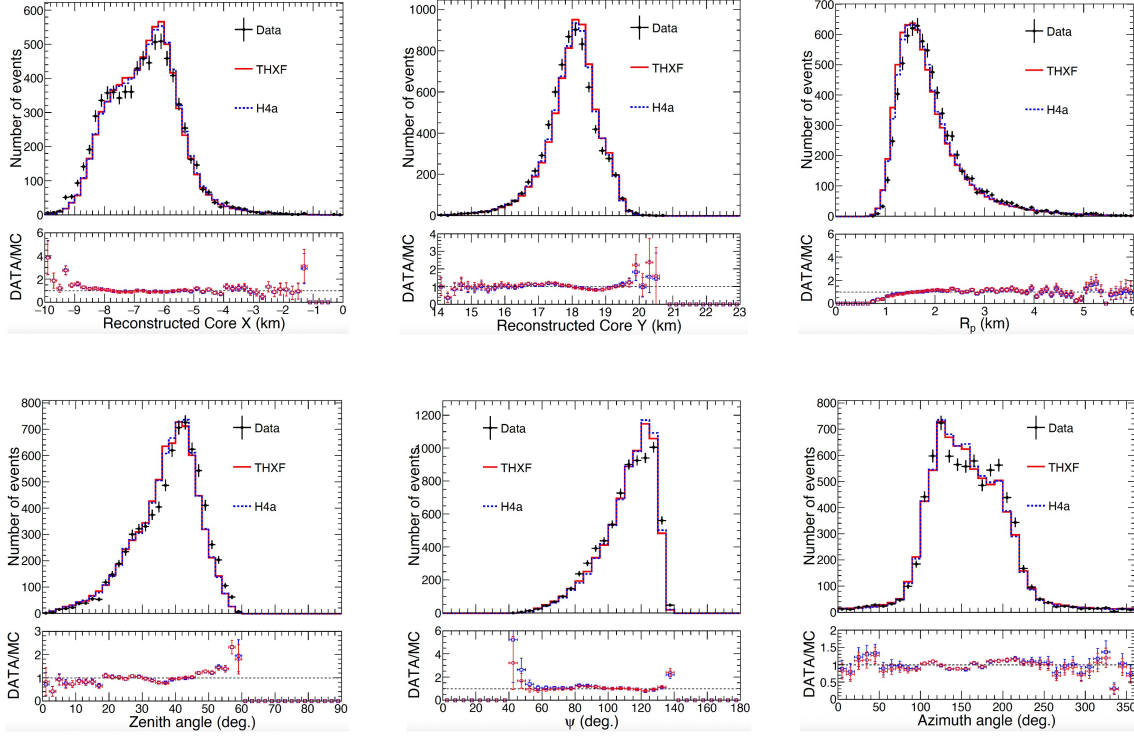


Figure 4: Distributions of reconstructed shower geometrical parameters. The figures show the X- and Y-projections of the shower core positions, R_p , Ψ , and zenith- and azimuth- angles of the shower axis. The data are shown by marker points, while the MC prediction are shown by the histograms for the THXF model and the H4a model, respectively. The MC predictions are normalized to the number of events in the data.

the preliminary results of the fundamental information and the energy spectrum with the TALE hybrid observation corresponding to the 1,247 hours of observation data. As a future prospect, it is expected that observations can be extended down to 10^{15} eV range through hybrid observations with the TALE infill SD array with 100 m spacing. Combining the TA and TAx4 as well as the TALE observation data, the energy spectrum is measured over five orders of magnitude from 10^{15} eV to 10^{20} eV. This energy spectrum measurement will play an important role in understanding the transition from cosmic rays of galactic origin to those of extragalactic origin.

Acknowledgements

The Telescope Array experiment is supported by the Japan Society for the Promotion of Science(JSPS) through Grants-in-Aid for Priority Area 431, for Specially Promoted Research JP21000002, for Scientific Research (S) JP19104006, for Specially Promoted Research JP15H05693, for Scientific Research (S) JP19H05607, for Scientific Research (S) JP15H05741, for Science Research (A) JP18H03705, for Young Scientists (A) JPH26707011, for Early-Career Scientists 25K17406, for Transformative Research Areas (A) JP25H01294, for International Collaborative Research 23KK0056, for International Collaborative Research 24KK0064, and for Fostering Joint International Research (B) JP19KK0074, by the joint research program of the Institute for Cosmic Ray Research (ICRR), The University of Tokyo; by the Pioneering Program of RIKEN for the Evolution of Matter in the Universe (r-EMU); by the U.S. National Science Foundation awards PHY-1806797, PHY-2012934, PHY-2112904, PHY-2209583, PHY-2209584, and PHY-2310163, as well as AGS-1613260, AGS-1844306, and AGS-2112709; by the National Research Foundation of Korea (2017K1A4A3015188, 2020R1A2C1008230, and RS-2025-00556637) ; by the Ministry of Science and Higher Education of the Russian Federation under the contract 075-15-2024-541, IISN project No.

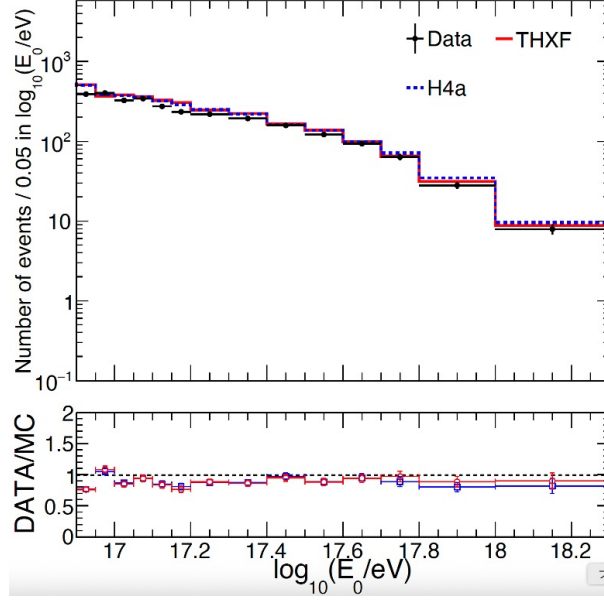


Figure 5: Comparisons of the measured energy distributions between the data and the MC predictions. The data are shown by marker points, while the MC prediction are shown by the histograms for the THXF model and the H4a model, respectively. The MC predictions are normalized to the number of events in the data.

4.4501.18, by the Belgian Science Policy under IUAP VII/37 (ULB), by National Science Centre in Poland grant 2020/37/B/ST9/01821, by the European Union and Czech Ministry of Education, Youth and Sports through the FORTE project No. CZ.02.01.01/00/22_008/0004632, and by the Simons Foundation (MP-SCMPS-00001470, NG). This work was partially supported by the grants of the joint research program of the Institute for Space-Earth Environmental Research, Nagoya University and Inter-University Research Program of the Institute for Cosmic Ray Research of University of Tokyo. The foundations of Dr. Ezekiel R. and Edna Wattis Dumke, Willard L. Eccles, and George S. and Dolores Doré Eccles all helped with generous donations. The State of Utah supported the project through its Economic Development Board, and the University of Utah through the Office of the Vice President for Research. The experimental site became available through the cooperation of the Utah School and Institutional Trust Lands Administration (SITLA), U.S. Bureau of Land Management (BLM), and the U.S. Air Force. We appreciate the assistance of the State of Utah and Fillmore offices of the BLM in crafting the Plan of Development for the site. We thank Patrick A. Shea who assisted the collaboration with much valuable advice and provided support for the collaboration's efforts. The people and the officials of Millard County, Utah have been a source of steadfast and warm support for our work which we greatly appreciate. We are indebted to the Millard County Road Department for their efforts to maintain and clear the roads which get us to our sites. We gratefully acknowledge the contribution from the technical staffs of our home institutions. An allocation of computing resources from the Center for High Performance Computing at the University of Utah as well as the Academia Sinica Grid Computing Center (ASGC) is gratefully acknowledged.

References

- [1] H. Kawai *et al.* (TA Collaboration), J. Phys. Soc. Jpn. Suppl. A **78**, 108 (2009).
- [2] T. Abu-Zayyad *et al.* (TA Collaboration), Astrophys. J. Lett. **768**, L1 (2013).
- [3] R. U. Abbasi *et al.* (TA Collaboration), PoS (ICRC2023) 379.
- [4] R. U. Abbasi *et al.* (TA Collaboration), Astrophys. J. **909**, 178 (2021).
- [5] D. Heck, G. Schatz, T. Thouw, J. Knapp, and J.N. Capdevielle, Tech. Rep. FZKA **6019** (1998).

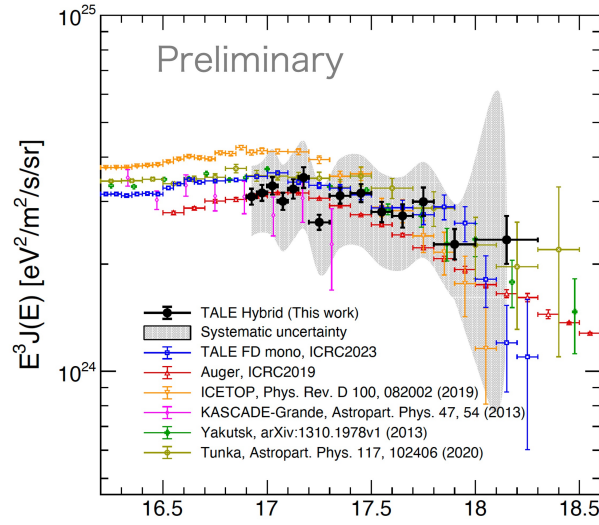


Figure 6: The result of energy spectrum. The spectrum obtained in this analysis is shown by the black data points. The error bars indicate the statistical uncertainties, while the gray band represents the systematic uncertainties. A mixed primary composition given by the THXF is assumed in this work.

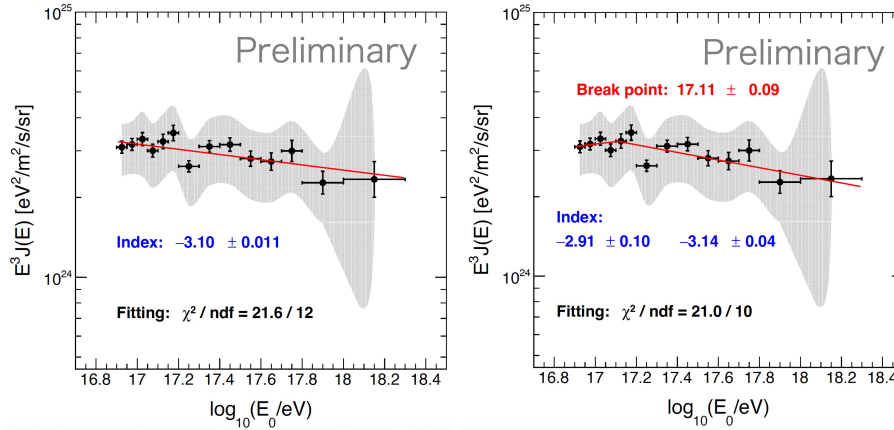
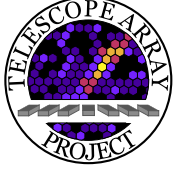


Figure 7: The results of energy spectrum with single and broken power-law fittings.

- [6] S. Ostapchenko, Nucl. Phys. B, Proc. Suppl. **151**, 143 (2006).
- [7] T. K. Gaisser, Astropart. Phys. **35**, 801 (2012).
- [8] K. Fujita *et al.* (TA Collaboration), PoS (ICRC2023) **401** (2023).
- [9] S. Agostinelli *et al.*, Nucl. Instrum. Methods Phys. Res., Sect. A **506**, 250 (2003).
- [10] J. Allison *et al.*, IEEE Trans. Nucl. Sci. **53**, 270 (2006).
- [11] J. Allison *et al.*, Nucl. Instrum. Methods Phys. Res., Sect. A **835**, 186 (2016).
- [12] T. Abu-Zayyad *et al.* (TA Collaboration), Nucl. Instrum. Methods Phys. Res. A **689**, 87 (2012).
- [13] G. D'Agostini, Nucl. Instrum. Methods Phys. Res., Sect. A **362**, 487 (1995).
- [14] G. D'Agostini, arXiv:1010.0632
- [15] K. Fujita, Ph.D. thesis, Osaka City University (2022).

Full Authors List: The Telescope Array Collaboration

R.U. Abbasi¹, T. Abu-Zayyad^{1,2}, M. Allen², J.W. Belz², D.R. Bergman², F. Bradfield³, I. Buckland², W. Campbell², B.G. Cheon⁴, K. Endo³, A. Fedynitch^{5,6}, T. Fujii^{3,7}, K. Fujisue^{5,6}, K. Fujita⁵, M. Fukushima⁵, G. Furlich², A. Gálvez Ureña⁸, Z. Gerber², N. Globus⁹, T. Hanaoka¹⁰, W. Hanlon², N. Hayashida¹¹, H. He^{12*}, K. Hibino¹¹, R. Higuchi¹², D. Ikeda¹¹, D. Ivanov², S. Jeong¹³, C.C.H. Jui², K. Kadota¹⁴, F. Kakimoto¹¹, O. Kalashev¹⁵, K. Kasahara¹⁶, Y. Kawachi³, K. Kawata⁵, I. Kharuk¹⁵, E. Kido⁵, H.B. Kim⁴, J.H. Kim², J.H. Kim^{2*}, S.W. Kim^{13*}, R. Kobo³, I. Komae³, K. Komatsu¹⁷, K. Komori¹⁰, A. Korochkin¹⁸, C. Koyama⁵, M. Kudenko¹⁵, M. Kuroiwa¹⁷, Y. Kusumori¹⁰, M. Kuznetsov¹⁵, Y.J. Kwon¹⁹, K.H. Lee⁴, M.J. Lee¹³, B. Lubsandorzhiev¹⁵, J.P. Lundquist^{2,20}, H. Matsushita³, A. Matsuzawa¹⁷, J.A. Matthews², J.N. Matthews², K. Mizuno¹⁷, M. Mori¹⁰, S. Nagataki¹², K. Nakagawa³, M. Nakahara³, H. Nakamura¹⁰, T. Nakamura²¹, T. Nakayama¹⁷, Y. Nakayama¹⁰, K. Nakazawa¹⁰, T. Nonaka⁵, S. Ogio⁵, H. Ohoka⁵, N. Okazaki⁵, M. Onishi⁵, A. Oshima²², H. Oshima⁵, S. Ozawa²³, I.H. Park¹³, K.Y. Park⁴, M. Potts², M. Przybylak²⁴, M.S. Pshirkov^{15,25}, J. Remington^{2*}, C. Rott², G.I. Rubtsov¹⁵, D. Ryu²⁶, H. Sagawa⁵, N. Sakaki⁵, R. Sakamoto¹⁰, T. Sako⁵, N. Sakurai⁵, S. Sakurai³, D. Sato¹⁷, K. Sekino⁵, T. Shibata⁵, J. Shikita³, H. Shimodaira⁵, H.S. Shin^{3,7}, K. Shinozaki²⁷, J.D. Smith², P. Sokolsky², B.T. Stokes², T.A. Stroman², H. Tachibana³, K. Takahashi⁵, M. Takeda⁵, R. Takeishi⁵, A. Taketa²⁸, M. Takita⁵, Y. Tameda¹⁰, K. Tanaka²⁹, M. Tanaka³⁰, M. Teramoto¹⁰, S.B. Thomas², G.B. Thomson², P. Tinyakov^{15,18}, I. Tkachev¹⁵, T. Tomida¹⁷, S. Troitsky¹⁵, Y. Tsunesada^{3,7}, S. Udo¹¹, F.R. Urban⁸, M. Vrábel²⁷, D. Warren¹², K. Yamazaki²², Y. Zhezher^{5,15}, Z. Zundel², and J. Zvirzdin²

¹ Department of Physics, Loyola University-Chicago, Chicago, Illinois 60660, USA

² High Energy Astrophysics Institute and Department of Physics and Astronomy, University of Utah, Salt Lake City, Utah 84112-0830, USA

³ Graduate School of Science, Osaka Metropolitan University, Sugimoto, Sumiyoshi, Osaka 558-8585, Japan

⁴ Department of Physics and The Research Institute of Natural Science, Hanyang University, Seongdong-gu, Seoul 426-791, Korea

⁵ Institute for Cosmic Ray Research, University of Tokyo, Kashiwa, Chiba 277-8582, Japan

⁶ Institute of Physics, Academia Sinica, Taipei City 115201, Taiwan

⁷ Nambu Yoichiro Institute of Theoretical and Experimental Physics, Osaka Metropolitan University, Sugimoto, Sumiyoshi, Osaka 558-8585, Japan

⁸ CEICO, Institute of Physics, Czech Academy of Sciences, Prague 182 21, Czech Republic

⁹ Institute of Astronomy, National Autonomous University of Mexico Ensenada Campus, Ensenada, BC 22860, Mexico

¹⁰ Graduate School of Engineering, Osaka Electro-Communication University, Neyagawa-shi, Osaka 572-8530, Japan

¹¹ Faculty of Engineering, Kanagawa University, Yokohama, Kanagawa 221-8686, Japan

¹² Astrophysical Big Bang Laboratory, RIKEN, Wako, Saitama 351-0198, Japan

¹³ Department of Physics, Sungkyunkwan University, Jang-an-gu, Suwon 16419, Korea

¹⁴ Department of Physics, Tokyo City University, Setagaya-ku, Tokyo 158-8557, Japan

¹⁵ Institute for Nuclear Research of the Russian Academy of Sciences, Moscow 117312, Russia

¹⁶ Faculty of Systems Engineering and Science, Shibaura Institute of Technology, Minumaku, Tokyo 337-8570, Japan

¹⁷ Academic Assembly School of Science and Technology Institute of Engineering, Shinshu University, Nagano, Nagano 380-8554, Japan

¹⁸ Service de Physique Théorique, Université Libre de Bruxelles, Brussels 1050, Belgium

¹⁹ Department of Physics, Yonsei University, Seodaemun-gu, Seoul 120-749, Korea

²⁰ Center for Astrophysics and Cosmology, University of Nova Gorica, Nova Gorica 5297, Slovenia

²¹ Faculty of Science, Kochi University, Kochi, Kochi 780-8520, Japan

²² College of Science and Engineering, Chubu University, Kasugai, Aichi 487-8501, Japan

²³ Quantum ICT Advanced Development Center, National Institute for Information and Communications Technology, Koganei, Tokyo 184-8795, Japan

²⁴ Doctoral School of Exact and Natural Sciences, University of Lodz, Lodz, Lodz 90-237, Poland

²⁵ Sternberg Astronomical Institute, Moscow M.V. Lomonosov State University, Moscow 119991, Russia

²⁶ Department of Physics, School of Natural Sciences, Ulsan National Institute of Science and Technology, UNIST-gil, Ulsan 689-798, Korea

²⁷ Astrophysics Division, National Centre for Nuclear Research, Warsaw 02-093, Poland

²⁸ *Earthquake Research Institute, University of Tokyo, Bunkyo-ku, Tokyo 277-8582, Japan*

²⁹ *Graduate School of Information Sciences, Hiroshima City University, Hiroshima, Hiroshima 731-3194, Japan*

³⁰ *Institute of Particle and Nuclear Studies, KEK, Tsukuba, Ibaraki 305-0801, Japan*

* Presently at: Purple Mountain Observatory, Nanjing 210023, China

* Presently at: Physics Department, Brookhaven National Laboratory, Upton, NY 11973, USA

* Presently at: Korea Institute of Geoscience and Mineral Resources, Daejeon, 34132, Korea

* Presently at: NASA Marshall Space Flight Center, Huntsville, Alabama 35812, USA